

Collisional dynamics of ultra-cold atomic gases

JEAN DALIBARD

Laboratoire Kastler-Brossel, 24 rue Lhomond, 75005 Paris, France

Collision physics plays a key role in understanding the properties of ultracold gases. First, collisions ensure thermalization in trapped atomic samples, which is essential for the success of evaporative cooling. Second, interactions between atoms determine the equilibrium shape and the dynamics of the condensate once it is formed. Finally collisions limit the achievable spatial densities *via* inelastic processes, which ultimately determine whether a given atomic species may lead to Bose-Einstein condensation.

The purpose of the following lectures is to give a basic introduction to collision physics with a special emphasis on the low temperature aspect of these interactions. We will consider here only binary interactions between atoms since one of the remarkable properties of the physics of ultra-cold dilute gases is that all the macroscopic properties of the system can be directly deduced from the two-body interaction potential. In particular the essential concept of *scattering length* will be introduced and developed for some simple potentials, using as practical examples experimental results obtained on atomic cesium and rubidium.

The present lectures are complementary to the ones given by D. Heinzen where a detailed comparison between the collisional properties of the various alkali atoms will be found, together with explanations of the spectroscopic approaches used in the precise determination of interatomic potentials.

1. – Scattering theory: a brief reminder

1.1. *Collision between two particles.* – We consider here an elementary collision process between two particles 1 and 2 with the same mass M , interacting through the potential

$V(\mathbf{r}_1 - \mathbf{r}_2)$. The Hamiltonian of the system is therefore

$$\hat{H} = \frac{\hat{p}_1^2}{2M} + \frac{\hat{p}_2^2}{2M} + V(\hat{\mathbf{r}}_1 - \hat{\mathbf{r}}_2) \quad .$$

Rather than working with these six degrees of freedom, we use the position and momentum operators for the center-of-mass ($\hat{\mathbf{R}}_G$ and $\hat{\mathbf{P}}_G$) and for the relative variable ($\hat{\mathbf{r}}$ and $\hat{\mathbf{p}}$):

$$(1) \quad \begin{cases} \hat{\mathbf{R}}_G &= (\hat{\mathbf{r}}_1 + \hat{\mathbf{r}}_2)/2 \\ \hat{\mathbf{P}}_G &= \hat{\mathbf{p}}_1 + \hat{\mathbf{p}}_2 \end{cases} \quad \begin{cases} \hat{\mathbf{r}} &= \hat{\mathbf{r}}_1 - \hat{\mathbf{r}}_2 \\ \hat{\mathbf{p}} &= (\hat{\mathbf{p}}_1 - \hat{\mathbf{p}}_2)/2 \end{cases} \quad .$$

The Hamiltonian can then be written:

$$\hat{H} = \frac{\hat{P}_G^2}{4M} + \frac{\hat{p}^2}{M} + V(\hat{\mathbf{r}}) \quad .$$

As expected, the center of mass moves as a free particle with a mass $2M$. The interesting collisional dynamics arises from the relative motion which corresponds to the scattering of a particle (the so-called *relative particle*) with reduced mass $m_r = M/2$ by the potential $V(\hat{\mathbf{r}})$. This is the problem that we now tackle.

1.2. The scattering amplitude. – To investigate the scattering properties of $V(\mathbf{r})$, we look for the eigenstates of the Hamiltonian of the relative motion with a well defined positive energy $E_k = \hbar^2 k^2 / (2m_r)$:

$$(2) \quad \left(\frac{\hat{p}^2}{2m_r} + V(\hat{\mathbf{r}}) \right) \psi_{\mathbf{k}}(\mathbf{r}) = E_k \psi_{\mathbf{k}}(\mathbf{r}) \quad ,$$

where we assume that $V(\mathbf{r})$ goes to zero when $|\mathbf{r}|$ goes to infinity.

We note b the range of action⁽¹⁾ of $V(\mathbf{r})$. For $|\mathbf{r}| \gg b$, we look for a solution of (2) with the following asymptotic form:

$$(3) \quad \psi_{\mathbf{k}}(\mathbf{r}) \sim e^{i\mathbf{k} \cdot \mathbf{r}} + f(k, \mathbf{n}, \mathbf{n}') \frac{e^{ikr}}{r} \quad ,$$

where $\mathbf{n} = \mathbf{k}/k$, $\mathbf{n}' = \mathbf{r}/r$. The physical meaning of this *collision state* is clear. It is the superposition of an incident plane wave with momentum \mathbf{k} (first part of (3)) and of a scattered wave function (second part of (3)). At a given point \mathbf{r} , the *scattering amplitude* $f(k, \mathbf{n}, \mathbf{n}')$ depends on the energy of the particle through k , and on the incident direction \mathbf{n} and the observation direction \mathbf{n}' (see figure 1).

⁽¹⁾ For potentials which are zero outside a certain volume this definition is obvious. For other potentials, decreasing for instance as r^{-6} (Van der Waals interaction) at infinity, the range will be defined quantitatively in the following.

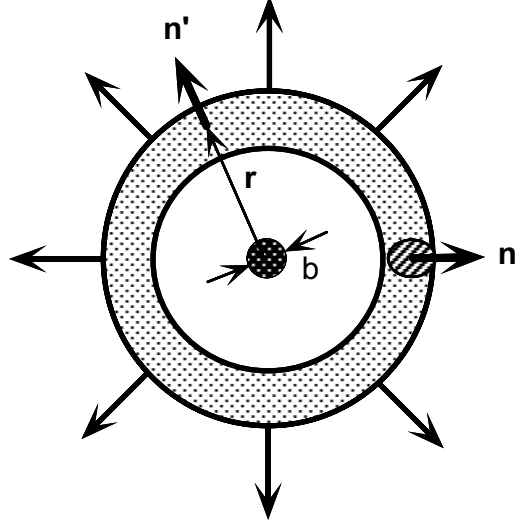


Fig. 1. – Scattering of an incident wave packet propagating along the direction \mathbf{n} by a potential $V(\mathbf{r})$ with a range b .

The central result of potential scattering is the following expression for the scattering amplitude (see *e.g.* [1, 2]):

$$(4) \quad f(k, \mathbf{n}, \mathbf{n}') = -\frac{m_r}{2\pi\hbar^2} \int e^{-i\mathbf{k}' \cdot \mathbf{r}'} V(\mathbf{r}') \psi_{\mathbf{k}}(\mathbf{r}') d^3r' \quad ,$$

where $\mathbf{k}' = k\mathbf{n}'$. This equation is implicit: it relates the value of the wave function $\psi_{\mathbf{k}}(\mathbf{r})$ (or, in other words, the scattering amplitude) far from the scattering region, to values of the same wave function inside the scattering region.

It is worth noting the following relation concerning the scattering amplitude:

$$(5) \quad f(k, \mathbf{n}, \mathbf{n}') = f(k, -\mathbf{n}', -\mathbf{n}) \quad ,$$

which arises from the time reversal symmetry of the problem [1].

From the value of the scattering amplitude one can then determine the differential and the total scattering cross-sections for this potential:

$$(6) \quad \frac{d\sigma}{d\Omega} = |f(k, \mathbf{n}, \mathbf{n}')|^2 \quad \sigma(k, \mathbf{n}) = \int |f(k, \mathbf{n}, \mathbf{n}')|^2 d^2n' \quad .$$

1.3. The low energy limit. – For small enough energies, the scattering process is isotropic, at least if the potential decreases fast enough at infinity. The energy scale below which this simplification occurs is directly related to the range b of the potential.

For $k \ll 1/b$ (or equivalently $E \ll \hbar^2/(2m_r b^2)$), the scattering amplitude is independent of the directions \mathbf{n} and \mathbf{n}' .

This essential result is quite clear from (4): the only \mathbf{r}' contributing to the integral are such that $|\mathbf{r}'| \leq b$. Therefore $|\mathbf{k}' \cdot \mathbf{r}'| \leq kb \ll 1$, so that one can replace $e^{-i\mathbf{k}' \cdot \mathbf{r}'}$ by 1, which means that the scattering amplitude is independent from the scattered direction \mathbf{n}' . Using (5), one then deduces that $f(k, \mathbf{n}, \mathbf{n}')$ is also independent from the incident direction \mathbf{n} .

Consequently, at low energy $E \ll \hbar^2/(2m_r b^2)$, the scattered wave is spherical:

$$\psi_{\mathbf{k}}(\mathbf{r}) \sim e^{i\mathbf{k} \cdot \mathbf{r}} + f(k) \frac{e^{ikr}}{r} \quad .$$

1.4. The Born approximation. – The complete analysis of the scattering problem requires the solution of the 3D Schrödinger equation which is often a tedious problem. Therefore it is very useful to derive a quick estimate of the scattering properties of a given potential using the Born approximation.

This approximation amounts to evaluate the scattering amplitude at first order in the potential V . In (4), one can then replace the exact unknown wave function $\psi_{\mathbf{k}}(\mathbf{r}')$ by the wave function at order zero in $V(r)$, *i.e.* $e^{i\mathbf{k} \cdot \mathbf{r}'}$. One is then left only with

$$(7) \quad f(k, \mathbf{n}, \mathbf{n}') = -\frac{m_r}{2\pi\hbar^2} \int e^{i(\mathbf{k}-\mathbf{k}') \cdot \mathbf{r}'} V(\mathbf{r}') d^3r' \quad ,$$

relating the scattering amplitude to the Fourier transform of the scattering potential $V(\mathbf{r})$. It is clear that such an approximation is meaningless for hard-core potentials, which take infinite values in some finite regions of space.

2. – Radial potentials and partial wave expansion

At this stage of our discussion, the exact determination of the scattering amplitude requires the solution of the three dimensional Schrödinger equation, which is quite tedious except for very particular cases. The situation is considerably simplified for the case of a spherically symmetric potential $V(\mathbf{r}) = V(r)$.

2.1. Scattering states and phase shifts. – For a radial potential $V(r)$, it is clear from symmetry arguments that the scattering amplitude depends only on the angle θ between the two unit vectors \mathbf{n} and \mathbf{n}' ($\cos\theta = \mathbf{n} \cdot \mathbf{n}'$) so that we will write in the following $f(k, \mathbf{n}, \mathbf{n}') \equiv f(k, \theta)$.

Let us denote z the direction of the incident wave function. To take advantage of the symmetry of the problem, it is convenient to expand the incident and scattered wave functions on a basis set of eigenfunctions of \hat{L}^2 and \hat{L}_z , where $\hat{\mathbf{L}}$ is the relative angular momentum:

$$(8) \quad \psi_{\mathbf{k}}(\mathbf{r}) = \sum_{l=0}^{\infty} \sum_{m=-l}^l Y_l^m(\theta, \phi) \frac{u_{k,l,m}(r)}{r} \quad ,$$

where ϕ is the azimuthal angle around the z axis and the $Y_l^m(\theta, \phi)$ are the spherical harmonic functions. The radial functions $u_{k,l,m}(r)$ are unknown at this stage.

Since the incident wave function is an eigenstate of \hat{L}_z with eigenvalue 0, the expansion of e^{ikz} is independent of the azimuthal angle around the z axis ($m = 0$) and one gets using standard angular momentum algebra:

$$(9) \quad e^{ikz} \sim \frac{1}{2ikr} \sum_{l=0}^{\infty} (2l+1) P_l(\cos \theta) \left((-1)^{l+1} e^{-ikr} + e^{ikr} \right) \quad \text{for } kr \gg 1 \quad ,$$

where the $P_l(\cos \theta)$ are the Legendre polynomials. Therefore the plane incident wave is a superposition of incoming waves $P_l(\cos \theta) e^{-ikr}/r$ and outgoing waves $P_l(\cos \theta) e^{ikr}/r$, with a relative phase 0 or π depending on the parity of l .

The scattering state $\psi_{\mathbf{k}}(\mathbf{r})$ is asymptotically the sum of the incident wave function and the outgoing wave $f(k, \theta) e^{ikr}/r$. It can therefore be written:

$$(10) \quad \psi_{\mathbf{k}}(\mathbf{r}) \sim \frac{1}{2ikr} \sum_{l=0}^{\infty} (2l+1) P_l(\cos \theta) \left((-1)^{l+1} e^{-ikr} + e^{2i\delta_l} e^{ikr} \right) \quad \text{for } |\mathbf{r}| \gg b \quad ,$$

where the coefficients $e^{2i\delta_l}$ have a modulus equal to 1, or equivalently, the phase shifts δ_l (defined here modulo π) are real. Indeed, due to the spherical symmetry of the potential, there is a conservation of the flux for each partial wave.

2.2. The 1D radial Schrödinger equation. – The solution of the scattering problem now amounts to the determination of the phase shifts $\delta_l(k)$. This is done by inserting the expression (8) into (2), which gives a 1D Schrödinger equation for each radial wave function $u_{k,l}(r)$ (we omit from now on the index $m = 0$). Assuming that $u_{k,l}(r)/r$ is regular in $r = 0$, this equation is:

$$(11) \quad u_{k,l}''(r) + \left(k^2 - \frac{l(l+1)}{r^2} - \frac{2m_r V(r)}{\hbar^2} \right) u_{k,l}(r) = 0 \quad .$$

According to (10), we choose the following asymptotic form for its solution:

$$(12) \quad u_{k,l}(r) \propto (-1)^{l+1} e^{-ikr} + e^{2i\delta_l} e^{ikr} \quad \text{for } r \gg b \quad .$$

The scattering amplitude $f(k, \theta)$ and the scattering cross-section $\sigma(k)$ are given by:

$$f(k, \theta) = \frac{1}{2ik} \sum_{l=0}^{\infty} (2l+1) (e^{2i\delta_l} - 1) P_l(\cos \theta)$$

and:

$$\sigma(k) = \sum_{l=0}^{\infty} \sigma_l(k) \quad \text{with} \quad \sigma_l(k) = \frac{4\pi}{k^2} (2l+1) \sin^2 \delta_l(k)$$

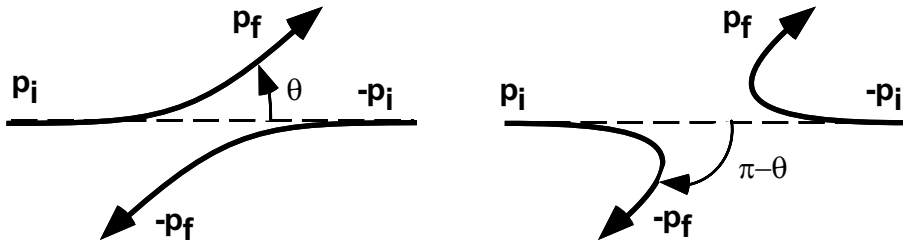


Fig. 2. – Two scattering processes leading to the same final state for indistinguishable particles.

Such a 1D problem can easily be solved numerically, if not analytically.

2'3. Identical particles. – Up to now, we have considered distinguishable particles assuming that we could discriminate (at least in principle) between the two scattering diagrams of figure 2, corresponding respectively to a scattering amplitude $f(k, \theta)$ and $f(k, \pi - \theta)$.

For identical particles, we have to take into account the (anti)symmetrisation principle which states that $\Psi(\mathbf{r}_1, \mathbf{r}_2) = \epsilon \Psi(\mathbf{r}_2, \mathbf{r}_1)$ where $\epsilon = +1$ (resp. -1) for polarized bosons (resp. fermions). Using

$$\Psi(\mathbf{r}_1, \mathbf{r}_2) = e^{i\mathbf{K}_G \cdot \mathbf{R}_G} \psi_{\mathbf{k}}(\mathbf{r}) \quad ,$$

where $\mathbf{R}_G = (\mathbf{r}_1 + \mathbf{r}_2)/2$ and $\mathbf{r} = \mathbf{r}_1 - \mathbf{r}_2$, we find that $\psi_{\mathbf{k}}(\mathbf{r}) = \epsilon \psi_{\mathbf{k}}(-\mathbf{r})$. The (anti)symmetrized scattering state can then be written asymptotically (for $\mathbf{k} \neq 0$):

$$(13) \quad \psi_{\mathbf{k}}(\mathbf{r}) \sim \frac{e^{ikz} + \epsilon e^{-ikz}}{\sqrt{2}} + \frac{f(k, \theta) + \epsilon f(k, \pi - \theta)}{\sqrt{2}} \frac{e^{ikr}}{r}$$

so that the differential cross-section reads:

$$(14) \quad \frac{d\sigma}{d\Omega} = |f(k, \theta) + \epsilon f(k, \pi - \theta)|^2 \quad ,$$

where θ varies in this case between 0 and $\pi/2$.

We now use the parity $(1)^l$ of spherical harmonic functions: the only partial waves contributing to the scattering cross-section for polarized bosons (resp. fermions) corresponds to even (resp. odd) values of l . The (anti)symmetrization principle therefore doubles the contribution of the even partial waves for bosons (the odd partial waves for fermions) and cancels the contribution of the odd ones (the even ones for fermions):

$$(15) \quad \text{Bosons:} \quad \sigma(k) = \frac{8\pi}{k^2} \sum_{l \text{ even}} (2l + 1) \sin^2 \delta_l(k) \quad ,$$

$$(16) \quad \text{Fermions:} \quad \sigma(k) = \frac{8\pi}{k^2} \sum_{l \text{ odd}} (2l + 1) \sin^2 \delta_l(k) \quad .$$

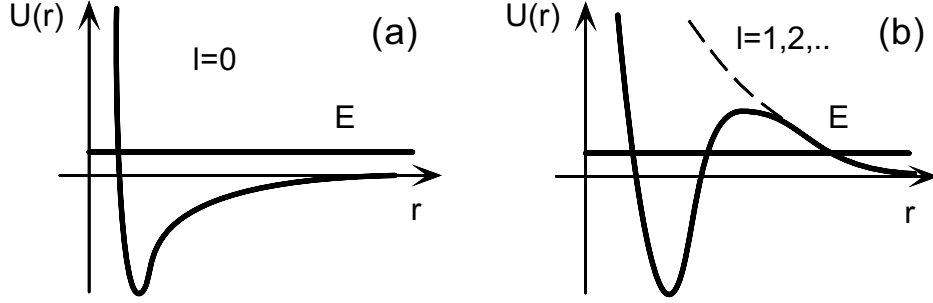


Fig. 3. – Potential entering into the 1D radial Schrödinger equation. (a) s -wave scattering. (b) scattering with $l > 0$; we have plotted in dotted line the centrifugal barrier $\hbar^2 l(l+1)/(2m_r r^2)$.

2.4. The low energy limit. – For the partial wave $l = 0$, the potential entering into the 1D Schrödinger equation (11) is simply the interatomic potential (figure 3a). For other partial waves, this potential is superimposed with the centrifugal barrier $\hbar^2 l(l+1)/(2m_r r^2)$ (figure 3b). In the latter case, the relative particle with an energy E much lower than the height of the resulting barrier will not “feel” the potential $V(r)$ and it will simply be reflected by the centrifugal barrier. We therefore expect qualitatively that the scattering due to $V(r)$ goes to zero for all partial waves but $l = 0$ at sufficiently low energy.

More precisely, one finds that [1, 2]:

$$(17) \quad \delta_l(k) \propto k^{2l+1} \quad \text{modulo } \pi \quad \text{when } k \rightarrow 0$$

so that the cross-section for the partial wave l is such that:

$$(18) \quad \sigma_{l \neq 0}(k) = \frac{8\pi}{k^2} (2l+1) \sin^2 \delta_l \propto k^{4l} \longrightarrow 0 \quad \text{when } k \rightarrow 0 \quad .$$

We recover the isotropy for low energy scattering that we had already found in the first section. The corresponding cross-section can be written:

$$(19) \quad \lim_{k \rightarrow 0} \sigma_{l=0}(k) = 8\pi a^2 \quad (\text{bosons}) \quad ,$$

where the *scattering length* a is defined by

$$(20) \quad a = - \lim_{k \rightarrow 0} \frac{\tan \delta_0(k)}{k} \quad .$$

An important consequence of this result is that polarized fermions do not “see” each other at low temperature. Indeed the scattering occurs only through partial waves $l = 1, 3, \dots$ whose cross-section tends to zero at low temperature. This makes the evaporative

cooling of a polarized fermionic gas quite difficult (see the contribution of G. Tino to this volume for possible remedies to this problem).

Remarks:

- The isotropy of low energy scattering is true only if the potential decreases fast enough at infinity. If it decreases as r^{-3} or slower, all partial waves contribute at low energy (see below and [1]).
- Even for Van der Waals potentials varying as r^{-6} , the statement (17) should be taken with care. Indeed for power law potentials $U(r) \propto r^{-n}$, (17) is valid only if $2l + 3 < n$, *i.e.* $l = 0$ or $l = 1$ for the Van der Waals potential ($n = 6$). For partial waves with $2l + 3 \geq n$, one finds $\delta_l(k) \propto k^{n-2}$ modulo π (see *e.g.* [1], §124).
- For $l \neq 0$, there might be some quasi-bound states in the potential well close to $r = 0$ (see figure 3b). There will then be a scattering resonance if the incident relative particle has an energy close to the energy of such a quasi-bound state, in complete analogy with the Fabry-Perot resonance in optics. These *shape resonances* may enhance strongly the contribution of $l \neq 0$ partial waves in an energy domain where one would have expected naively a pure $l = 0$ scattering [3].

2.5. Scattering length and mean field energy. – To end this section, let us emphasize the key role played by the concept of scattering length in the statistical physics description of cold gases in general, and of Bose-Einstein condensation in particular. Provided the gas is in the dilute regime ($n|a|^3 \ll 1$ where n is the spatial density), and assuming it is cold enough for the limit (19) to be valid, the many-body description of the gas can be shown to depend *only* on the scattering length and *not* on the detailed interatomic potential. In other words, two interatomic potentials corresponding to the same scattering length lead to the same properties for the condensed gas, although they may have completely different microscopic properties, one being attractive and the other one repulsive for instance.

We illustrate this result using a *refractive index* approach [4], by analyzing how a particle propagates in an atomic medium, assuming that the collisions occur at low energy so that the scattering state for a given collisionnal process can be written:

$$(21) \quad \psi_{\mathbf{k}}(\mathbf{r}) \sim e^{i\mathbf{k}\cdot\mathbf{r}} - \frac{a}{r} e^{ikr} \quad .$$

Suppose that a particle with momentum $\hbar\mathbf{K} \neq \mathbf{0}$ parallel to the z axis crosses at right angle a slab of thickness L containing scatterers at rest with a spatial density n (figure 4). We consider first the case where the incident particle has equal mass but is not identical to the scatterers. The scattering state for a single collision event between the particle (position \mathbf{r}_P) and a scatterer located in \mathbf{r}_1 , can be written using (1) and (21):

$$(22) \quad \Psi(\mathbf{r}_P, \mathbf{r}_1) = e^{iKz_P} - \frac{a}{|\mathbf{r}_P - \mathbf{r}_1|} e^{iK|\mathbf{r}_P - \mathbf{r}_1|/2} e^{iK(z_P + z_1)/2} \quad .$$

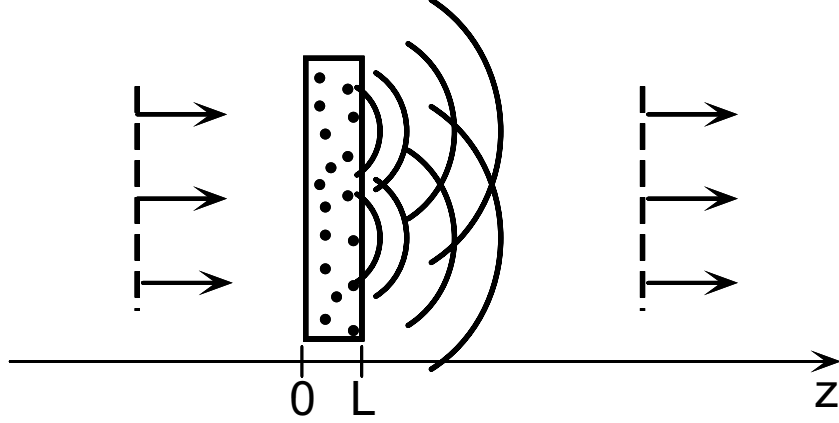


Fig. 4. – An incident particle with mass M crosses a slab containing scatterers with spatial density n . The transmitted wave is dephased with respect to the incident one by a phase shift proportionnal to the scattering length a . This phase shift can be interpreted as resulting from a potential energy $4\pi\hbar^2 an/M$ exerted by the slab onto the incident particle ($8\pi\hbar^2 an/M$ if the incident particle is identical to the particles in the slab).

Once the incident particle has crossed the slab, the state of the system is the superposition of the initial state and of all the scattered waves resulting from the collisions of the incident particle with the N atoms of the slab:

$$(23) \quad \Psi(\mathbf{r}_P, \mathbf{r}_1, \dots, \mathbf{r}_N) = e^{iKz_P} - \sum_{j=1}^N \frac{a}{|\mathbf{r}_P - \mathbf{r}_j|} e^{iK|\mathbf{r}_P - \mathbf{r}_j|/2} e^{iK(z_P + z_j)/2} .$$

For simplicity we neglect here multiple scattering events.

We now evaluate the transmitted wave by projecting the state of the system onto the subspace where all scatterers are still at rest:

$$(24) \quad \psi_T(z_P) = e^{iKz_P} - n \int \frac{a}{|\mathbf{r}_P - \mathbf{r}_1|} e^{iK|\mathbf{r}_P - \mathbf{r}_1|/2} e^{iK(z_P + z_1)/2} d^3r_1$$

where the integral over \mathbf{r}_1 is taken over the volume of the slab. Using cylindrical coordinates along the z -axis, this integral can be exactly calculated and we find at first order in the density n for $z > L$:

$$(25) \quad \psi_T(z_P) = Ae^{iKz_P} \quad \text{with} \quad A = 1 - i \frac{4\pi anL}{K} \simeq e^{-i4\pi anL/K} \quad (\text{Thin slab}).$$

This simple phase shift can be interpreted as a modification δK of the incident particle

wave vector when the particle is inside the slab:

$$(26) \quad \delta K = -\frac{4\pi a n}{K} \quad .$$

This change of momentum is equivalent to a change of kinetic energy inside the slab:

$$(27) \quad \delta \left(\frac{\hbar^2 K^2}{2M} \right) = -\frac{4\pi \hbar^2 a n}{M} \quad .$$

In other words, the slab creates on the incident particle a potential energy:

$$(28) \quad \textit{particle distinguishable from the scatterers:} \quad U = \frac{4\pi \hbar^2 a n}{M} \quad .$$

If a is positive, this potential energy is positive: the particle slows down as it enters the slab; the particle is effectively repelled from the slab. On the contrary, U is negative for a negative a : the incident particle is in this case attracted by the slab and it accelerates as it enters the slab.

Now, if the particle is identical to the scatterers, one has to symmetrize the initial state (22). The rest of the calculation proceeds along the same lines and one gets (as above) a result two times larger than for discernable particles:

$$(29) \quad \textit{particle identical to the scatterers:} \quad U = \frac{8\pi \hbar^2 a n}{M} \quad .$$

This potential is the one which appears when one considers the interaction between condensate and above condensate particles.

3. – The scattering length for some simple potentials

As shown above, for low enough energy, the collisions are essentially occurring in the s -wave regime, *i.e.* they correspond to an isotropic scattered wave. Moreover, when the relative wave vector k (or the energy $\hbar^2 k^2 / (2m_r)$) tends to zero, the phase shift $\delta_0(k)$ for s -wave is proportional to k (modulo π) so that the scattering amplitude tends to a constant:

$$f(k) \Big|_{s \text{ wave}} = \frac{e^{i\delta_0(k)} \sin \delta_0(k)}{k} \longrightarrow -a \quad \text{when} \quad k \rightarrow 0 \quad .$$

The solution of the scattering problem at ultra-low energies therefore amounts to the determination of a single quantity: the scattering length a .

Such a determination is in principle straightforward. We consider the 1D Schrödinger equation corresponding to s -waves ($l = 0$ in (11)), and we look for a solution of this equation with zero energy (putting $u_{k=0, l=0}(r) \equiv u(r)$ for simplicity):

$$(30) \quad u''(r) - \frac{2m_r V(r)}{\hbar^2} u(r) = 0 \quad ,$$

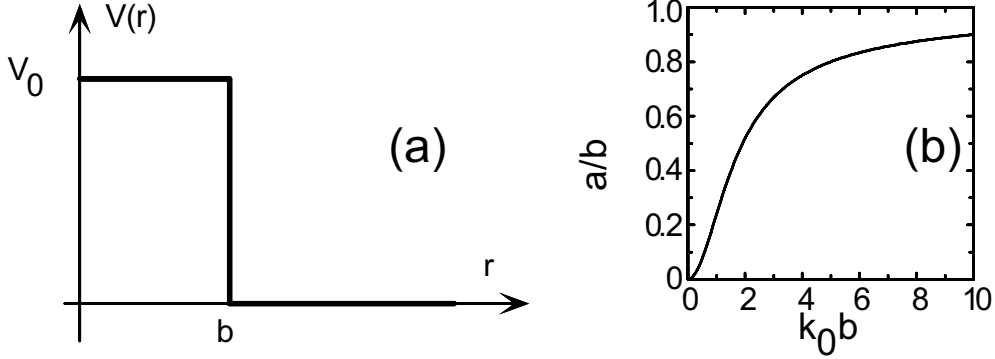


Fig. 5. – (a) Square potential barrier. (b) Scattering length as a function of $k_0 = \sqrt{2m_r U_0}/\hbar$. For large enough barriers (hard core potential), the scattering length is equal to the radius of the core.

and with the asymptotic behaviour deduced from (12):

$$u(r) \propto r - a \quad \text{for large } r \quad .$$

The physical meaning of the scattering length is then clear. Consider the scattering state $u_{k,l=0}(r)$ and its asymptotic value $\propto \sin(kr + \delta_0(k))$. This asymptotic value has a series of zeros $r_n(k) = (-\delta_0(k) + n\pi)/k$, where n is an integer. When k goes to zero, all the $r_n(k)$ go to $\pm\infty$, except for one which tends to a (which can be either positive or negative). An illustration of this will be given in fig.10 for the potential $V(r) = -C_6 r^{-6} + C_{12} r^{-12}$.

We now derive the value of the scattering length for some basic potentials before addressing in the next section the more realistic case of Van der Waals potentials.

3'1. The square potential barrier. – Consider the case of the square spherical barrier represented in fig. 5a, where $V(r) = V_0 > 0$ if $r \leq b$ and $V(r) = 0$ otherwise. The solution of (30) is then straightforward:

$$\begin{aligned} u(r) &= C_1 (r - a) & \text{for } r > b \\ u(r) &= C_2 \sinh(k_0 r) & \text{for } r \leq b \end{aligned} \quad ,$$

where we have put $k_0 = \sqrt{2m_r V_0}/\hbar$ and where C_1 and C_2 are normalizing coefficients.

The continuity of $u(r)$ and $u'(r)$ in $r = b$ then implies:

$$(31) \quad a = b - \frac{\tanh k_0 b}{k_0} \quad .$$

This result is plotted in figure 5b. The scattering length is always positive. For large enough barriers ($k_0 b \gg 1$ or equivalently $U_0 \gg \hbar^2/(2m_r b^2)$), we recover the hard sphere

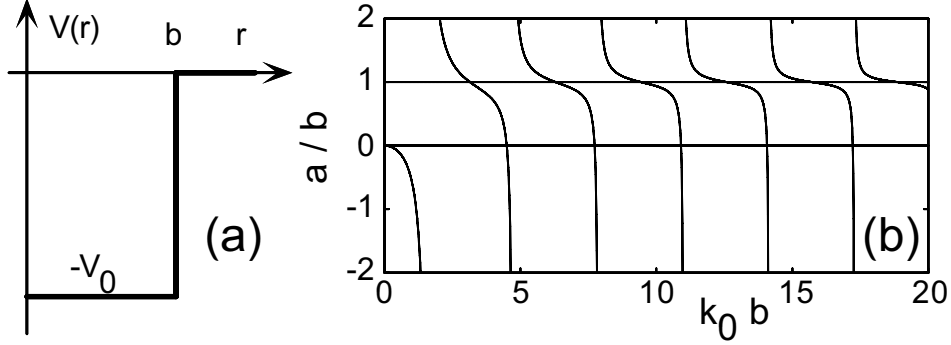


Fig. 6. – (a) Square potential well. (b) Scattering length as a function of $k_0 = \sqrt{2m_r U_0}/\hbar$. The scattering length can be positive or negative and it diverges for values of k_0 corresponding to the appearance of a new bound state in the well.

scattering problem; the scattering length in this case is just equal to the radius b of the hard sphere core.

3.2. The square potential well. – Consider now a square potential well such that $U(r) = -U_0$ for $r \leq b$ ($U_0 > 0$) and $U(r) = 0$ otherwise (figure 6a). The solution of (30) is:

$$\begin{aligned} u(r) &= C_1 (r - a) & \text{for } r > b \\ u(r) &= C_2 \sin(k_0 r) & \text{for } r \leq b \end{aligned} ,$$

from which we deduce:

$$(32) \quad a = b - \frac{\tan k_0 b}{k_0} .$$

The result (32) is plotted in fig. 6b. It is obviously more complicated than the result found for a square barrier and it is useful for the following to keep in mind the following remarks:

- For a small potential, *i.e.* $k_0 b < \pi/2$, the scattering length a is negative. The condition $k_0 b < \pi/2$ corresponds to the case where U_0 is too small to have a bound state in the potential well.
- If we increase continuously the well depth U_0 , we find that the scattering length goes to infinity when $k_0 b = \pi/2$, *i.e.* when the potential is large enough to hold a bound state. If we keep increasing U_0 , we find that such divergences occur for all values of U_0 such that $k_0 b = (2n + 1)\pi/2$, where n is an integer. Each of these discrete values of U_0 corresponds to the appearance of a new bound state in the potential well. This relation between the divergence of the scattering length

and the appearance of a bound state is quite general (Levinson theorem). These resonances leading to a divergence of the scattering length are called *zero-energy resonances*.

- When U_0 is slightly lower than the threshold for the appearance of a new bound state, the scattering length a is large and negative; if U_0 is slightly larger than this threshold, a is large and positive. This result is also general.
- Suppose that U_0 is large enough so that there is a large number of bound states ($k_0 b \gg 1$). Except for a very small domain of values of k_0 in the vicinity of zero-energy resonances, the scattering length a is positive and very close to the range b of the potential well. We are therefore led to the rather surprising result that a deep square potential well is very likely to have the same scattering properties as a large square potential barrier with equal range. This result is specific of square well potentials.

3.3. Contact interaction: the pseudo-potential. – *A priori* the simplest interaction between two particles is the contact interaction given by the potential:

$$V(\mathbf{r}_1 - \mathbf{r}_2) = g \delta(\mathbf{r}_1 - \mathbf{r}_2) \quad .$$

In particular, such a contact interaction is at the basis of the N -body approach to quantum gases. Let us consider how such a $\delta(\mathbf{r})$ potential can be handled in scattering theory.

If we just consider the limit of the two previous examples with U_0 going to infinity, b going to 0, and keeping the constant product $\frac{4\pi}{3} b^3 U_0 = g$, we find that the scattering length a goes to zero. We recover here the statement that often appears in Quantum Mechanics textbooks: “a 3D δ -potential does not lead to scattering”.

Remark: The Born approximation for the contact interaction **does not** lead to a zero result. From (7), we find a scattering amplitude $f_{\text{Born}} = -m_r g / (2\pi \hbar^2)$ which is independent of angle and energy. This result actually coincides with the zero-energy limit of the result obtained with the regularization of the contact potential that we now present.

A proper and non ambiguous way to deal with contact interaction is to use the pseudo-potential [5]:

$$(33) \quad V(\mathbf{r}) \psi(\mathbf{r}) = g \delta(\mathbf{r}) \frac{\partial}{\partial r} (r \psi(\mathbf{r})) \quad .$$

Let us comment briefly on this expression:

- If the wave function $\psi(\mathbf{r})$ is regular in $\mathbf{r} = \mathbf{0}$, this definition directly leads to:

$$(34) \quad \psi \text{ regular in } \mathbf{0} : \quad V(\mathbf{r}) \psi(\mathbf{r}) = g \psi(\mathbf{0}) \delta(\mathbf{r}) \quad ,$$

which is the expected result for a contact interaction.

- If the wave function belongs to a larger class of functions, namely if it can be written:

$$(35) \quad \psi(\mathbf{r}) = \frac{u(\mathbf{r})}{r} \quad ,$$

where $u(\mathbf{r})$ is regular in $\mathbf{r} = 0$, the action of V is still well defined:

$$(36) \quad \psi \text{ of the type of (35) : } \quad V(\mathbf{r})\psi(\mathbf{r}) = g \left(\frac{\partial u}{\partial r} \right)_{r=0} \delta(\mathbf{r}) \quad .$$

Note that the simple contact potential $g\delta(\mathbf{r})$ acting on such functions (with $u(\mathbf{0}) \neq 0$) would not give a sensible result, although these functions are perfectly admissible as quantum states (*e.g.* they can be normalized without problem).

We now solve the Schrödinger equation for the pseudo-potential keeping in mind that the class of solutions may include functions of the type (35). The expression of the Laplacian operator acting on this class of functions has to be modified with respect to what we used to write down (11). Using

$$\psi(\mathbf{r}) = \frac{u(\mathbf{0})}{r} + \frac{u(\mathbf{r}) - u(\mathbf{0})}{r} \quad ,$$

we obtain

$$(37) \quad \Delta\psi(\mathbf{r}) = -4\pi u(\mathbf{0})\delta(\mathbf{r}) + \frac{1}{r} \frac{\partial^2 u}{\partial r^2} - \frac{1}{\hbar^2 r^2} \hat{L}^2 \psi(\mathbf{r}) \quad .$$

For partial waves other than $l = 0$, one can easily check that the presence of the centrifugal potential imposes that the wave function $\psi(\mathbf{r})$ is regular and goes to 0 when \mathbf{r} goes to $\mathbf{0}$. Using (34), we then find that the pseudo-potential (33) has no effect for these partial waves.

We consider now s -wave scattering from the pseudo-potential, so that we choose a spherically symmetric wave function $\psi(r) = u(r)/r$. Inserting this wave function in the Schrödinger equation, we obtain:

$$(38) \quad -\frac{\hbar^2}{2m_r} \left(-4\pi u(0)\delta(\mathbf{r}) + \frac{u''(r)}{r} \right) + g\delta(\mathbf{r})u'(0) = \frac{\hbar^2 k^2}{2m_r} \frac{u(r)}{r} \quad .$$

Separating the terms regular in $r = 0$ and the terms proportional to $\delta(\mathbf{r})$, we obtain

$$(39) \quad u''(r) + k^2 u(r) = 0 \quad \quad u(0) = -\frac{gm_r}{2\pi\hbar^2} u'(0) \quad ,$$

from which we deduce the s -wave scattering amplitude $f(k)$ for any k and its relation with the scattering length:

$$(40) \quad f(k) = -\frac{a}{1 + ika} \quad \text{with} \quad a = \frac{gm_r}{2\pi\hbar^2} = \frac{gM}{4\pi\hbar^2}$$

Since there is no scattering in partial waves other than the s -wave, the scattering state is now completely determined:

$$(41) \quad \psi_{\mathbf{k}}(\mathbf{r}) = e^{i\mathbf{k}\cdot\mathbf{r}} - \frac{a}{1 + ika} \frac{e^{ikr}}{r} \quad .$$

For the pseudo-potential, we find that the scattering length is directly proportional to the strength g of the potential. Therefore the Born approximation coincides with the zero-energy limit. This remarkable property greatly simplifies the treatment of the N -body problem for ultra-cold gases, when one models the atom-atom interaction with this pseudo-potential.

The total cross section for polarized bosons is easily derived from the previous results:

$$(42) \quad \sigma(k) = \frac{8\pi a^2}{1 + k^2 a^2} \quad ,$$

which leads to the two asymptotic results for small and large k 's:

$$(43) \quad \begin{cases} ka \ll 1 & \sigma(k) \simeq 8\pi a^2 \\ ka \gg 1 & \sigma(k) \simeq 8\pi/k^2 \end{cases} \quad .$$

The first line is just the usual result for ultra-low energy (19), while the second line expresses the fact that at high energy, the cross-section reaches the maximal value allowed for s -wave scattering (15): this is the so-called *unitary limit*.

4. – Van der Waals potentials

Up to now, we have only considered model potentials, which are rather far from the real interaction which takes place between two neutral atoms. We now turn to the more realistic case of a long range r^{-6} interaction corresponding to the Van der Waals potential.

We will follow here the treatment of Gribakin and Flambaum who have considered the case of a truncated r^{-6} potential (figure 7a):

$$(44) \quad \begin{cases} V(r) = +\infty & \text{if } r < r_c \\ V(r) = -C_6/r^6 & \text{if } r \geq r_c \end{cases} \quad .$$

Of course such a potential does not describe properly the short range interaction of the two atoms, but, as we show below, this does not change the main features of the scattering properties at low energy.

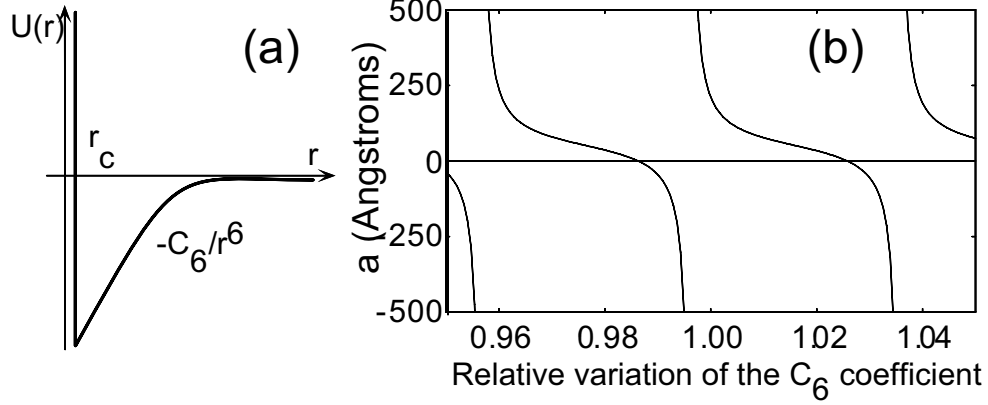


Fig. 7. – (a) Truncated Van der Waals potential. (b) Variations of the scattering length a for a small change of the C_6 coefficient (parameters for the cesium atom).

4.1. *Characteristic length and energy for s -wave scattering.* – The Schrödinger equation for s wave scattering ($l = 0$ in 11) can be cast in a dimensionless form:

$$(45) \quad u'' + \left(\frac{1}{\rho^6} + (ka_c)^2 \right) u = 0 \quad u(\rho_c) = 0 \quad ,$$

where we have introduced the characteristic length:

$$(46) \quad a_c = \left(\frac{2m_{\text{T}}C_6}{\hbar^2} \right)^{1/4} \quad ,$$

and where we have put:

$$\rho = r/a_c \quad \rho_c = r_c/a_c \quad .$$

The length a_c gives the typical scale for the scattering length, as we show below.

Consider as an example the case of cesium atoms (^{133}Cs) prepared in the doubly (electron+nucleus) polarized state ($F = m_F = 4$). If we neglect the weak magnetic dipole couplings, the atoms interact in this case only through the *triplet* potential. The C_6 coefficient is $C_6 = 6.6 \cdot 10^{-76} \text{ J.m}^{-6}$ [6] and the minimum of the triplet potential occurs for a distance equal to $\sim 6 \text{ \AA}$. We choose an r_c close to this value. The value of the characteristic length a_c is quite large, $a_c = 107 \text{ \AA}$, so that $\rho_c \ll 1$. This allows the replacement of the solutions of (45) (Bessel functions for $k = 0$) by their asymptotic values [7].

The length a_c also enters in the determination of the energy range where s -wave scattering is dominant. Consider the total (Van der Waals + centrifugal potential) for

d -waves (p -wave scattering does not exist for polarized bosons)

$$V_{\text{eff}}(r) = -\frac{C_6}{r^6} + \frac{3\hbar^2}{m_r r^2} \quad .$$

The height of the potential barrier due to the centrifugal force is then found to be $2\sqrt{2}\hbar^2/(m_r a_c^2)$, corresponding to a relative distance $r = a_c/2^{1/4}$. Comparing this barrier height with the incident energy $\hbar^2 k^2/(2m_r)$, we find that for $ka_c < 2$, the scattering occurs essentially in s -waves (except for possible shape resonances), while for $ka_c > 2$ partial waves with higher angular momentum must be taken into account.

4.2. *The scattering length.* – In order to derive the scattering length a for the truncated Van der Waals potential, we put as before $k = 0$ in (45) and we look for a solution varying asymptotically as $r - a$. This procedure is described in detail in [7] so that we simply give here the result:

$$(47) \quad a \simeq \tilde{a}_c (1 - \tan \Phi) \quad ,$$

where \tilde{a}_c is directly proportionnal to a_c :

$$(48) \quad \tilde{a}_c = \frac{\Gamma(3/4)}{2\sqrt{2}\Gamma(5/4)} a_c \simeq 0.478 a_c \quad ,$$

and where the angle Φ depends on the hard core position:

$$(49) \quad \Phi = \frac{a_c^2}{2r_c^2} - \frac{3\pi}{8} \quad .$$

The result (47) is valid when $\Phi \gg 1$, which is indeed the case for cesium atoms ($\Phi \simeq 140$). This validity condition requires that there are several bound states in the potential well, since this number (equal to the number of divergences of a – Levinson theorem –) is given by Φ/π .

The quasi-periodic variations of a with the C_6 coefficient obtained using (47) are plotted in fig. 7b. One sees that a depends critically on C_6 (or on the hard core position), since a change of 4 % of C_6 is sufficient to introduce a new bound state in the potential well and to change continuously a from $+\infty$ to $-\infty$. The type of variations given in fig. 7 are actually quite general. If one uses a softer core around $r = 0$ such as C_{12}/r^{12} , one recovers a quasi-identical figure with again an extreme sensitivity to the value of the C_6 coefficient and to the core parameters.

For cesium atoms, the present knowledge of the interatomic atomic potential is not sufficient to determine accurately the value of Φ (modulo π) and therefore to derive the scattering length from (47). However this result has some virtues. First it shows that if we assume a random distribution for Φ (the best way to express our ignorance...), the probability for having a positive scattering length is 3/4 ($n\pi < \Phi < (n + 3/4)\pi$). This

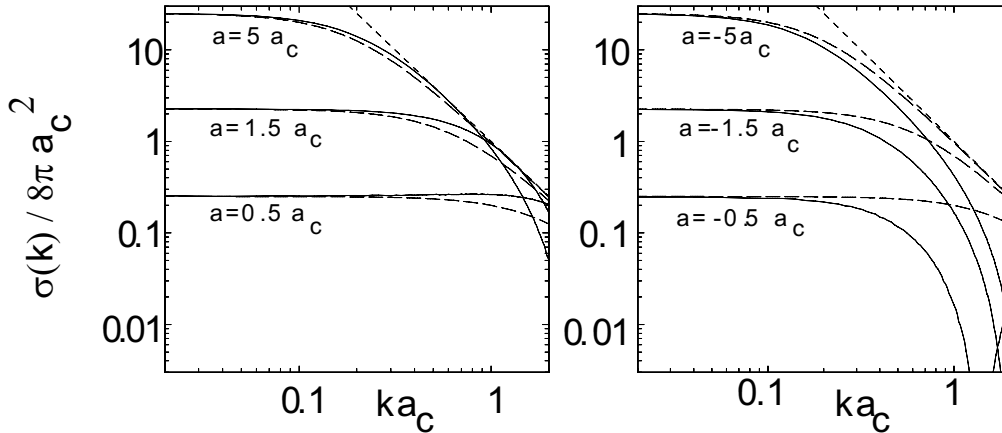


Fig. 8. – Variations of the s -wave cross section $\sigma_0(k)$ for the truncated Van der Waals potential with $\rho_c \approx 0.06$. The exact value of ρ_c is adjusted to obtain $a/a_c = \pm 0.5, \pm 1.5, \pm 5$. We restrict ourselves to k values such that $k < 2a_c^{-1}$, corresponding to the range where s -wave scattering is dominant. With short-dashed line we indicate the unitary limit $\sigma_{\text{unit}}(k) = 8\pi/k^2$ and with long-dashed lines the results from the pseudo-potential approach $8\pi a^2/(1 + k^2 a^2)$.

has to be contrasted with the case of the square well where a is very likely to be positive if there are a large number of bound states in the well. Second it gives the natural scale \tilde{a}_c (50 Å for Cs) for the scattering length. One sees that this “typical value” is much larger than the size of an atom (a few Å at most).

4.3. The s -wave cross-section as a function of incident energy. – For the description of a Bose-Einstein condensate, it is usually sufficient to know the scattering length associated with the interatomic potential. Indeed the temperatures corresponding to the BEC transition are low enough to ensure that the s -wave phase shift $\delta_0(k)$ varies as $-ak$ over the range of relevant relative wave vectors.

For the optimization of the evaporation sequences that (may) lead to the condensation, one needs more informations on the atom-atom interactions. In particular one should know the variations of the total cross-section with temperature (or with k). In this paragraph, we outline the important features of these variations for the truncated Van der Waals potential, keeping in mind that our conclusions are actually valid for other types of core potentials as long as the long range part r^{-6} remains unchanged.

We concentrate here on the s -wave scattering since it is usually the relevant energy domain over which evaporation is performed. We have plotted in fig. 8 the results for $\sigma_0(k)$ for various scattering lengths a : $a/a_c = \pm 0.5, \pm 1.5, \pm 5$. These different values of a were obtained by varying slightly the core radius ρ_c around 0.06, which is typical for cesium atoms (actually, very similar curves are obtained for a core radius twice as large). The value of the s -wave phase shift is obtained using a numerical integration of

(45) from the core radius up to values of r where the potential is negligible ($r > 300a_c$). The following points concerning fig. 8 should be emphasized:

- As expected, the s -wave cross-section tends to $8\pi a^2$ when k tends to zero.
- For positive values of a (left side of fig.8), the cross-section is close to the result $8\pi a^2/(1 + k^2 a^2)$ plotted in dashed lines. It is therefore a relatively good approximation to replace the unknown cross-section by the one calculated for the pseudo-potential.
- For negative a 's, the pseudo-potential result is a poorer approximation of $\sigma_0(k)$. One notes in particular that for $a/a_c = -0.5$ or -1.5 , there is a value of k below $2a_c^{-1}$ for which $\sigma_0(k)$ is zero. The mathematical reason for this vanishing cross-section $\sigma_0(k) = (8\pi/k^2) \sin^2 \delta_0(k)$ lies in the k -dependence of $\delta(k)$. For very low k , $\delta(k) \sim -ak$ (modulo π) is positive. However, for $ka \sim 1$, the variations of $\delta(k)$ do not depend on the precise value of a (at least if $|a|$ is not too large) and are approximately $\delta(k) \sim -a_c k$, leading to negative values for the phase shift. Therefore there is a value $k \leq 1/a_c$ where the phase shift $\delta_0(k)$ is zero, leading to a zero-scattering length. Such a zero-scattering length makes the evaporative cooling of the gas quite difficult, since the thermalization rate around this point becomes very long (see [3] for the discussion of this point for the particular case of ^{85}Rb).

5. – The case of $1/r^3$ potential

As we already mentioned, the partial wave analysis and the asymptotic laws (17) and (18) are valid only if the potential $V(r)$ decreases fast enough at infinity. In particular, if $V(r)$ decreases as $1/r^3$ or slower, the differential scattering cross-section is not isotropic anymore even in the limit of a zero-energy: all partial waves contribute even for $k = 0$.

This can be seen clearly if we consider a truncated r^{-3} potential [1]:

$$(50) \quad \begin{aligned} V(r) &= -C_3/r^3 & r > b \\ V(r) &= 0 & r \leq b \end{aligned}$$

that we treat within the Born approximation:

$$\begin{aligned} f(k, \mathbf{n}, \mathbf{n}') &\simeq -\frac{m_r}{2\pi\hbar^2} \int e^{i(\mathbf{k}-\mathbf{k}')\cdot\mathbf{r}'} V(\mathbf{r}') d^3r' \\ &= \frac{2m_r C_3}{\hbar^2} \int_{|\mathbf{k}-\mathbf{k}'|b}^{\infty} \frac{\sin u}{u^2} du \\ &\sim -\frac{2m_r C_3}{\hbar^2} \log(|\mathbf{k}-\mathbf{k}'|b) \quad . \end{aligned}$$

The result, which diverges logarithmically for low energy, is clearly non-isotropic. One can extract from it a characteristic length a_c :

$$(51) \quad a_c = \frac{2m_r C_3}{\hbar^2}$$

which gives the typical “scattering length” for such a problem.

Such a r^{-3} potential is not just an academic counterexample. Since the alkali atoms used in low temperature atomic physics have a permanent magnetic moment, two atoms interact together with the standard dipole-dipole coupling:

$$(52) \quad V(\mathbf{r}) = \frac{\mu_0}{4\pi r^3} (\boldsymbol{\mu}_1 \cdot \boldsymbol{\mu}_2 - 3(\boldsymbol{\mu}_1 \cdot \mathbf{u})(\boldsymbol{\mu}_2 \cdot \mathbf{u})) \quad ,$$

where $\mathbf{r} = \mathbf{r}_1 - \mathbf{r}_2$ and $\mathbf{u} = \mathbf{r}/r$. Although this potential is not as simple⁽²⁾ as (50), we can still get an order of magnitude of its scattering properties by putting in (51) the corresponding value for C_3 : $C_3 = \mu_0 \mu_B^2 / (4\pi)$, where μ_B is the Bohr magneton. After a simple algebra, we get

$$\frac{a}{a_{\text{Bohr}}} \sim \frac{1}{4} \alpha^2 \frac{M}{m_e} \quad ,$$

where m_e is the electron mass.

The role of this potential might be important for the evaporative cooling of fermions. As we already pointed out, the elastic cross-section for polarized fermions tends to zero at low temperature if the atoms interact through a “standard” potential decreasing fast enough at infinity (*e.g.* Van der Waals). On the contrary, for the magnetic dipole-dipole interaction, the cross-section does not tend to zero even for polarized fermions and this interaction can in principle lead to a significant evaporative cooling for Fermi gases.

For ${}^6\text{Li}$, the formula given above leads to $a_c \sim 0.1 a_{\text{Bohr}}$, which is clearly too small to be useful (the corresponding cross-section would be 10^6 smaller than for ${}^{87}\text{Rb}$ atoms for instance). However, for atoms with a larger mass and a larger magnetic dipole moment, this effect might be a significant help to achieve ultra-low temperatures for Fermi systems. Let us also mention the recent theoretical work of Marinescu and You, who have suggested to apply a static electric field to the system in order to polarize the atoms and take benefit of an electric dipole-dipole interaction [9].

6. – How can one measure a scattering length?

The *ab initio* calculation of the scattering length from the knowledge of the interatomic potential is usually not possible. Except for atomic hydrogen, the potentials for alkali atoms are not known precisely enough to compute accurately a .

The most precise way to determine a is based on spectroscopic measurements, where one measures the position of the highest bound levels in the interatomic potential. This method, photoassociation spectroscopy, is described in detail in [3]. Note that it may be

⁽²⁾ For the dipole-dipole potential, assuming that all magnetic moments are parallel to each other, as it is the case in a magnetic trap, the Born approximation result does not lead to the logarithmic divergence found for the isotropic r^{-3} potential, but it gives a finite result (see *e.g.* [8]).

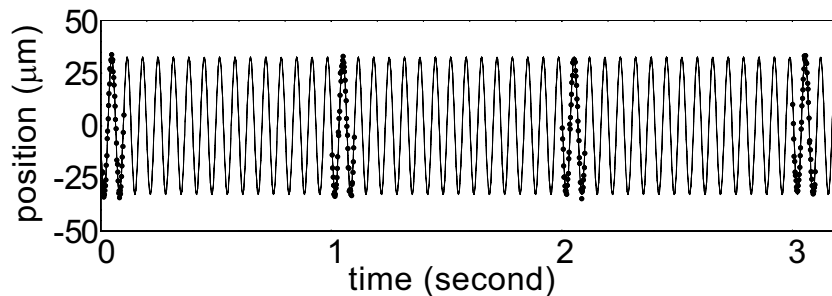


Fig. 9. – Undamped oscillations of the center of mass of a rubidium cloud along one of the axes of a harmonic magnetic trap. The continuous line is a sinusoidal fit to the experimental data. The temperature of the cloud is $T = 250$ nK and there are 2.5×10^6 atoms. The collision rate is $\sim 2.6 \text{ s}^{-1}$. From such a set of data, one can determine very precisely the oscillation frequency ($14.87 (\pm 0.01)$ Hz in this case). These data have been obtained by J. Söding, D. Guéry-Odelin, P. Desbiolles, and F. Chevy.

difficult to apply to some chemical elements. For instance, until very recently [10], no photoassociation data was available for atomic cesium.

A “macroscopic” way to determine the elastic cross-section, *i.e.* the absolute value of a , is to monitor the collisional dynamics of an atomic cloud confined in a trap. The cloud is prepared out of thermal equilibrium and one compares the relaxation time towards equilibrium with the predictions of a molecular-dynamics simulation.

It is worth noting that not all deviations from thermal equilibrium lead to relaxation. Let us give two examples for this somehow subtle point. Consider first a cloud trapped in a harmonic potential and suppose that the center of mass of the cloud is displaced from the center of the trap. One might naively expect that the center of mass will undergo an oscillation damped by atomic collisions. This is not the case. Assuming for simplicity an isotropic trap with frequency $\omega/(2\pi)$ and using the Hamiltonian:

$$H = \sum_{i=1}^N \left(\frac{p_i^2}{2M} + \frac{1}{2} M \omega^2 r_i^2 \right) + \frac{1}{2} \sum_{i,j} V(\mathbf{r}_i - \mathbf{r}_j) \quad ,$$

one can easily check that the evolutions of the center-of-mass position \mathbf{R} and momentum \mathbf{P} are given by:

$$\dot{\mathbf{R}} = \mathbf{P}/M_T \quad \dot{\mathbf{P}} = -M_T \omega^2 \mathbf{R}$$

where M_T is the total mass $M_T = NM$. These two equations do not depend on the interatomic potential and do not present any damping, as shown in figure 9.

The other undamped motion concerns the monopole oscillation in an isotropic harmonic trap [11]. Suppose that one starts with a classical gas at thermal equilibrium and that one changes suddenly the spring constant of the trap. One might expect that

the breathing mode which is excited in this way should be damped after a few collision times, allowing thus a measurement of this collision time. This is not the case and one can check, at least within the description of the gas dynamics by the Boltzmann equation, that this mode oscillates with no damping at the frequency $2\omega/(2\pi)$.

Except for these two singular situations, the thermal relaxation in a harmonic trap provides a simple way to evaluate scattering cross-sections. The cloud should be prepared with a small deviation from equilibrium and one should concentrate on the longest time constant for the relaxation process. A typical procedure is to prepare the cloud with an average energy which is not the same along the three principal axes of the harmonic trap [12, 13, 14] and to monitor the redistribution of energy among the three axes.

Consider for instance a TOP trap [15] for which one expects at equilibrium $\langle x^2 \rangle = \langle y^2 \rangle = 8\langle z^2 \rangle$, where z is the axis of the quadrupole field of the TOP trap. The deviation from equilibrium is produced by radio frequency evaporation which ejects atoms located outside a volume close to a cylinder around the z axis. Therefore one produces in this way a cloud with $\langle x^2 \rangle = \langle y^2 \rangle < 8\langle z^2 \rangle$. From a numerical simulation based on molecular dynamics, one finds that the relaxation time to equilibrium is of the order⁽³⁾ of $3 \gamma_c^{-1}$, where the collision rate γ_c is defined by:

$$\gamma_c = \bar{n} \bar{v} \sigma \quad \bar{n} = \frac{\int n^2(\mathbf{r}) d^3r}{\int n(\mathbf{r}) d^3r} \quad \bar{v} = \frac{4}{\sqrt{\pi}} \sqrt{\frac{kT}{M}} .$$

Here \bar{n} stands for the average density in the trap ($\bar{n} = n_0/(2\sqrt{2})$ for a Gaussian distribution, n_0 being the density at center) and \bar{v} is the average relative collision velocity.

The average density and the temperature are determined from the absorption image of the cloud in the trap. From the measurement of γ_c , one can then deduce the value of σ . Note that this approach is valid if the cross-section is constant for all relevant relative velocities inside the thermal distribution of the cloud. In presence of a zero-energy resonance, as it is the case for the cesium atom in the doubly polarized state, this approach has to be modified in order to take into account the variations of σ with the relative momentum k of the colliding atoms [14].

7. – Elastic *vs.* inelastic processes

Up to now, we have neglected inelastic collisions. As long as this is legitimate, the achievement of Bose-Einstein condensation in a trapped sample is just a matter of time. By setting the evaporation barrier well above the thermal energy $k_B T$, atoms with high energy, produced via binary elastic collisions, will continuously leave the trap, and the phase space density of the remaining gas will increase: the BEC threshold will then eventually be reached. Unfortunately, inelastic processes which constitute an additionnal loss of atoms from the trap may render this achievement much more difficult.

⁽³⁾ More precisely, the relaxation time varies from $2.4 \gamma_c^{-1}$ to $3.4 \gamma_c^{-1}$, when the collision rate γ_c varies from $0.01\omega_x$ (collision less regime) to ω_x (hydrodynamic regime) (see also [16]).

7.1. *The three classes of inelastic processes.* –

- Collisions of trapped atoms with background gas: these processes induce an exponential decay of the number of trapped atoms, $\dot{N} = -N/\tau$. Their role can be reduced by improving the quality of vacuum. The trap lifetime τ is typically one or several minutes. The condition for achieving runaway evaporation (increase of the collision rate as the evaporation proceeds) is $\gamma_c\tau > 140$, where γ_c is the collision rate at the beginning of evaporation [17, 18, 19].
- Two-body spin dipolar relaxation (see *e.g.* [20, 21, 22]): the atoms in a magnetic trap are confined with their magnetic moment antiparallel to the local magnetic field (low-field seeking states). Indeed the trap is centered around a magnetic field minimum, and the interaction of atoms with the field is: $W = -\boldsymbol{\mu}\cdot\mathbf{B}(\mathbf{r}) = +\mu B(\mathbf{r})$. Now the magnetic interaction between two trapped atoms, given by (52), may lead to a spin flip of one or of the two colliding atoms. This is energetically favourable since it corresponds to a release of energy⁽⁴⁾ of the order of $\mu B(\mathbf{r})$.
- Three-body recombination (see *e.g.* [23, 24, 21]): when three trapped atoms are close enough, two of them may form a molecule, the third one carrying away the released momentum and energy. For trapped alkali atoms, this process plays only a minor role for uncondensed clouds. For instance, for ^{87}Rb in its low hyperfine state, the measured rate is $K_3 = 4 \times 10^{-29} \text{ cm}^6\text{s}^{-1}$ [25], so that the corresponding decay rate is smaller than 1/minute as long as the peak density in the trap does not exceed $5 \times 10^{13} \text{ cm}^{-3}$. On the contrary, these processes constitute an essential source of losses for Bose-Einstein condensates [25].

7.2. *The case of atomic cesium.* – The magnitude of inelastic processes varies very much from one atom to the other. In Paris, we have investigated in detail during the past few years the case of ^{133}Cs . This atom is of particular interest because the hyperfine splitting between its two ground sublevels (angular momentum $F = 3$ and $F = 4$) is at the basis of time and frequency standards. The achievement of a Cs BEC could lead to a significant improvement of these standards. In addition Cs was initially considered to be a very good candidate for BEC experiments [26].

Our setup is based on a double magneto-optical trap (MOT) system, ensuring both an efficient loading of the magnetic trap (10^8 atoms in ~ 2 seconds) and a good vacuum at the location of this trap ($< 10^{-10}$ mbar) [14]. Our results concerning both hyperfine states $F = 3$ and $F = 4$ have been described in detail in recent publications so that we only briefly outline them here.

For both hyperfine states, we have measured a large elastic cross section, corresponding to a scattering length larger in absolute value than 140 \AA for the upper hyperfine

⁽⁴⁾ If the atoms are trapped in their upper hyperfine state, one or both atoms may emerge from the collision in the lower hyperfine state; the energy gain is then much larger, equal to the hyperfine splitting.

state [14], and larger than 300 Å for the lower state [27]. This is much larger than the “typical” scattering length expected from the cesium C_6 coefficient (eqs. 46-48): $\tilde{a}_c \simeq 50$ Å. The occurrence of such a quasi zero-energy resonance (see §3.2) is at first sight very favourable for the achievement of BEC, since even a modest initial spatial density should be sufficient to provide a large elastic collision rate and a strong evaporation.

Unfortunately for the achievement of BEC, we have also found, for both hyperfine states, large inelastic rates due to two-body processes. This limited the maximal phase-space density achievable in our experiment to $\sim 10^{-2}$. Let us briefly describe as an example the measurement performed on the lower hyperfine state $F = -m_F = 3$ [28]. Using radio-frequency evaporation, we prepared at time $t = 0$ an atomic cloud at a well defined temperature. We then let the cloud sit in the trap with a “radio-frequency shield” for a variable time. The radio-frequency allows to choose the effective trap depth such that any atom having undergone a spin flip collision (gain of energy $\propto \mu B$) escapes from the trap. From the decay of the number of trapped atoms as a function of time we can deduce the two-body inelastic collision rate. For a field $B = 10^{-4}$ T and a temperature $T = 1$ μ K we measure a two-body rate $\sim 4 \times 10^{-13}$ cm³s⁻¹, which is at least two orders of magnitude larger than for lighter alkalis such as Na or ⁸⁷Rb. For the upper hyperfine state the measured two-body rate is even larger (4×10^{-12} cm³s⁻¹ at the lowest temperature obtained for this state, *i.e.* 8 μ K) [29].

Several physical reasons can be invoked to explain such large dipolar rates (for recent quantitative theoretical accounts of the Cs experimental results, see [30, 31]).

First the large value for the scattering length enhances the occupation probability at short distances for the low-energy collisional states of two Cs atoms. This favors any inelastic process occurring at such short distances. An example of this effect is shown in fig. 10, where we consider a potential varying as $-C_6 r^{-6} + C_{12} r^{-12}$. The C_6 coefficient is equal to the value for Cs given above; the C_{12} coefficient is adjusted to give a minimum of the interatomic potential around 6.4 Å, as for the real Cs-Cs interaction. A fine tuning of this C_{12} coefficient allows one to vary the scattering length. In fig. 10, we have chosen three values of C_{12} , corresponding either to a “normal” scattering length, $a = +50$ Å, or to “large” scattering lengths, $a = \pm 500$ Å, and we have plotted the corresponding scattering states. It is clear from this figure that, for the same normalization at infinity, the amplitude of the scattering state at short interatomic distances is increased by a factor ~ 10 (*i.e.* 500 Å / 50 Å) in the case of the large scattering lengths. This corresponds to an increase by a factor 100 of the occupation probability at such short distances, where inelastic processes are likely to take place.

Second there exists, in addition to the standard dipole-dipole interaction (52), an extra spin-spin coupling, arising as a second-order effect in the electronic spin-orbit coupling [22]. For heavy alkali such as Cs, this extra coupling can actually play a more important role than the standard magnetic dipole-dipole interaction.

Finally, as pointed out in [30], a Feshbach resonance occurs in collisions between cesium atoms prepared in the state $F = 3$, for a magnetic field of the order of a few 10^{-4} T. This resonance is responsible for the enhancement of both the elastic and inelastic rates for the lower hyperfine state.

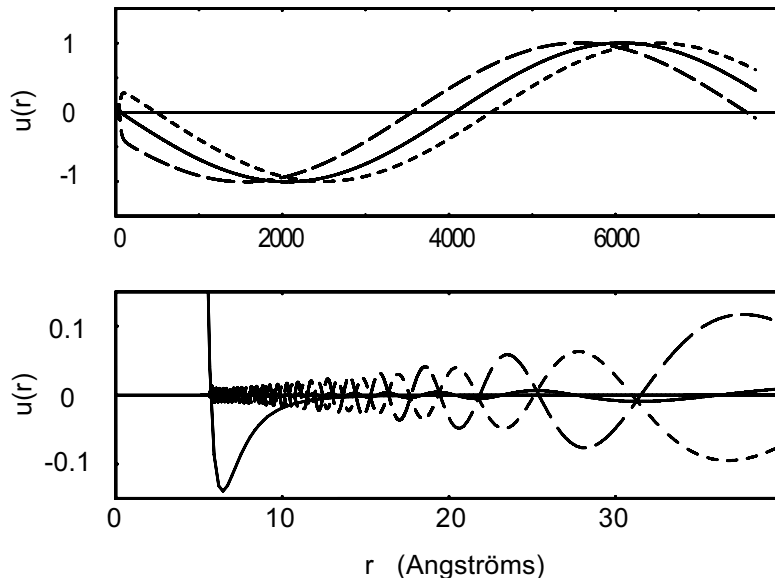


Fig. 10. – Scattering states in a $-C_6r^{-6} + C_{12}r^{-12}$ potential. The C_6 and C_{12} have been chosen to match the long range part and the position of the minimum of the Cs-Cs potential. With a fine tuning of the C_{12} coefficient, we adjust the scattering length to be equal to 50 Å –continuous line– (the \tilde{a}_c value of (48)), to -500 Å–long dashed line–, and to $+500$ Å–short dashed line–. We have plotted low energy scattering states, with the same normalization at infinity. For large scattering lengths ($|a| = 500$ Å) the probability for having the two colliding atoms close together is strongly enhanced.

To summarize, the achievement of BEC with ^{133}Cs in a magnetic trap seems quite difficult. For atoms prepared in the upper, doubly polarized ground level ($F = 4$) spin-dipole relaxation induces hyperfine-changing collisions which prevent reaching a regime of efficient evaporative cooling. For atoms prepared in the lower hyperfine state ($F = 3$), one should run the magnetic trap at a bias field much smaller than the usual ones, which are around 10^{-4} T, so that the energy gain μB in a spin flip will be reduced. We have tried to run our magnetic trap with such a reduced bias field (10^{-5} T); unfortunately, the lifetime τ of our sample was then considerably shortened ($\tau \sim 5$ s), preventing us from achieving an efficient evaporative cooling. We think that this limitation was due to technical magnetic noise, and that it could be circumvented in a carefully shielded apparatus.

Two other options are possible to get a cesium BEC. The first one is to confine the ^{133}Cs atoms in the lowest state $m_F = 3$ of the $F = 3$ manifold by using a laser or a hybrid laser-magnetic trap⁽⁵⁾. In this case no binary inelastic process can occur, and the

(⁵) We recall that it is not possible to trap this high-field seeking state in a pure magnetic trap,

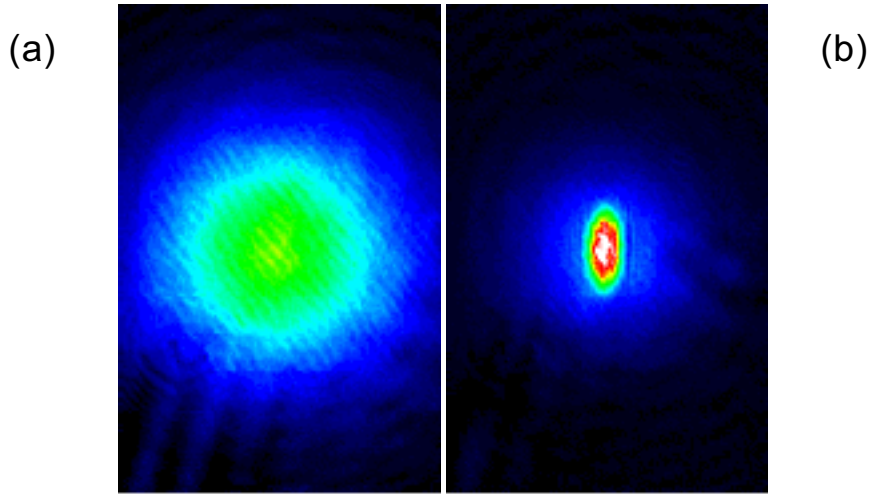


Fig. 11. – Velocity distributions of a ^{87}Rb gas. Both pictures represent the absorption of a probe laser beam by the cloud after a 31 ms free fall. (a) Temperature above condensation: isotropic velocity distribution. (b) Temperature below condensation: the anisotropic central feature corresponds to a macroscopically occupied ground state. This figure was obtained by P. Desbiolles, D. Guéry-Odelin, and J. Söding.

only limitations to the achievement of BEC will lie in the 3-body recombination process, whose rate is currently unknown [32]. The scattering length for this state has recently been predicted to be negative except for some particular values of the magnetic field [30]. The achievement of a ^{133}Cs BEC in such a trap and the study of the size of the condensate as a function of B would therefore constitute a very stringent test of our understanding of Cs-Cs cold collisions. The other option is to turn to another isotope of cesium, ^{135}Cs . The predicted scattering length is positive and the dipolar relaxation rate should be much smaller than for ^{133}Cs [30].

7.3. The case of atomic rubidium. – Fortunately not all alkali atoms behave like ^{133}Cs with respect to ultra-cold collisions, and it is now well known that evaporative cooling of ^{87}Rb , ^7Li , and ^{23}Na can lead to BEC [33, 34, 35].

Because of the similarities of the physical properties of Cs and Rb, it was relatively easy to convert our experimental setup from one atomic species to the other. Keeping the same vacuum setup and the same magnetic trap technology, we have achieved in our double MOT system the loading of 10^9 ^{87}Rb atoms in the magnetic trap (oscillation frequencies $\nu_x = 15.0$ Hz, $\nu_y = \nu_z = 244$ Hz). After a 15 second radio-frequency evaporation ramp, we reach the BEC threshold for a temperature 0.6 μK . The transition is observed

since one cannot produce a local maximum of magnetic field in vacuum.

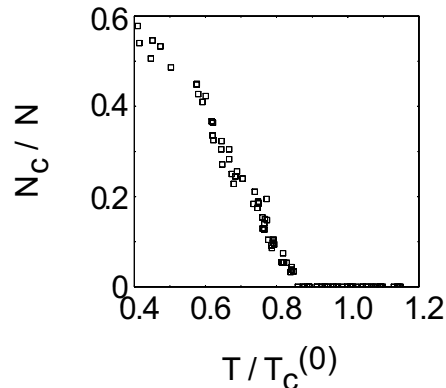


Fig. 12. – Variations of the condensed fraction N_c/N , as a function of temperature, scaled by the transition temperature for the ideal gas $T_c^{(0)}$ (Data from J. Söding, D. Guéry-Odelin, P. Desbiolles, F. Chevy, and I. Inamori).

by a standard time-of-flight technique, which gives the momentum distribution of the trapped gas [33]. Above the transition, the momentum distribution is approximately isotropic; below the transition, a strongly anisotropic feature appears at the center of the distribution, reflecting the anisotropy of the confining potential, as shown in figure 11.

The number of atoms at the transition point is in our setup $\sim 3 \times 10^6$. In order to analyze precisely our data, we follow a procedure similar to [36]. We determine the temperature T of the cloud by fitting the wings of the uncondensed part of the velocity distribution by a Gaussian function. The number of atoms in the condensate (N_c) is determined by fitting the central component with an inverted paraboloidal distribution, corresponding to the Thomas-Fermi solution of the Gross-Pitaevski equation describing the condensate, after the TOF expansion [37]. Finally the total number of atoms N is determined from the integrated absorption of the cloud. The condensate fraction N_c/N is plotted in fig. 12 as a function of $T/T_c^{(0)}$ (where $T_c^{(0)}$ is the critical temperature for the ideal Bose-Einstein distribution). The clouds with no apparent condensed fraction were fitted using a single Gaussian distribution. We measure a transition temperature $T_c \simeq 0.86 (\pm 0.10) T_c^{(0)}$, in good agreement with the predictions of [38] ($T_c/T_c^{(0)} = 0.91$).

8. – Conclusion

We have presented in this set of lectures the basics elements for understanding the collisions which take place between ultra-cold atoms. This presentation is far from being exhaustive. In particular we have not addressed the possible control of the collisional properties of an atomic gas using light, or an electric or magnetic dc-field. We have also addressed only briefly the complex problem of inelastic processes, taking as an example the cesium atom; a more complete treatment of this problem would require a whole set

of lectures for itself. We hope however that these notes may be helpful as an introduction to this fascinating and lively subject of research.

Acknowledgments: I would like to thank warmly the ENS BEC team, Pierre Desbiolles, David Guéry-Odelin and Johannes Söding, whose work has been presented here. The help of Markus Arndt and Maxime Ben Dahan at the early stage of the Cs experiment, and the recent contributions of Jean-Christophe Antona, Frédéric Chevy and Itoshi Inamori on the Rb setup have also been very valuable. Finally I would like to acknowledge many helpful discussions with Y. Castin, C. Cohen-Tannoudji, C. Salomon, P. Julienne, G. Shlyapnikov, and S. Stringari.

Laboratoire Kastler Brossel is a *unité de recherche de l'ENS et de l'Université Pierre et Marie Curie, associée au CNRS*. This work was partially funded by EC (TMR network ERB FMRX-CT96-0002), Collège de France and DRED.

REFERENCES

- [1] L. D. Landau and E. M. Lifshitz, *Quantum Mechanics*, §131, Pergamon Press, Oxford (1977).
- [2] C. J. Joachain, *Quantum collision theory*, p. 78-105 (1983), North-Holland, Amsterdam.
- [3] D. Heinzen, contribution to this volume.
- [4] The same result can be derived from other points of view: see the contributions of K. Burnett, S. Fetter and A. Griffin to this volume.
- [5] K. Huang, *Statistical Mechanics*, (Wiley, New York, 1987) and references in.
- [6] W. Weickenmeier, U. Diemer, M. Wahl, M. Raab, and W. Demtröder, *J. Chem. Phys.* **82**, 5354 (1985).
- [7] G. F. Gribakin and V. V. Flambaum, *Phys. Rev. A* **48**, 546 (1993).
- [8] G. V. Shlyapnikov, J. T. M. Walraven, U. M. Rahmanov, and M. W. Reynolds, *Phys. Rev. Lett.* **73**, 3247 (1994).
- [9] M. Marinescu and L. You, preprint (march 1998).
- [10] A. Fioretti, D. Comparat, A. Crubellier, O. Dulieu, F. Masnou-Seeuws, and P. Pillet, *Phys. Rev. Lett.* **80**, 4402 (1998).
- [11] L. Boltzmann, *Wissenschaftliche Abhandlungen*, Vol. II ; G. E. Uhlenbeck and G. W. Ford, *Lectures in Statistical Mechanics*, American Mathematical Society (Providence, 1963).
- [12] C. R. Monroe, E. A. Cornell, C. A. Sackett, C. J. Myatt, and C. E. Wieman, *Phys. Rev. Lett.* **70**, 414 (1993).
- [13] K. B. Davis, M.-O. Mewes, M. A. Joffe, M. R. Andrews, and W. Ketterle, *Phys. Rev. Lett.* **74**, 5202 (1995).
- [14] M. Arndt, M. Ben Dahan, D. Guéry-Odelin, M. W. Reynolds, and J. Dalibard, *Phys. Rev. Lett.* **79**, 625 (1997).
- [15] W. Petrich, M. H. Anderson, J. R. Ensher, and E. A. Cornell, *Phys. Rev. Lett.* **74**, 3352 (1995).
- [16] H. Wu and C. J. Foot, *J. Phys. B.* **29**, L321 (1996).
- [17] J. T. M. Walraven, *Proc. Scott. Univ. Summer Sch. Phys.* **44**.
- [18] O. J. Luiten, M. W. Reynolds, and J. T. M. Walraven, *Phys. Rev. A* **53**, 381 (1996).
- [19] W. Ketterle and N. J. Van Druten, *Advances in Atomic, Molecular, and Optical Physics*, **37**, 181 (1996).

- [20] H. Boesten, A. J. Moerdijk, and B. J. Verhaar, *Phys. rev. A* **54**, R29 (1996).
- [21] A. J. Moerdijk and B. J. Verhaar, *Phys. Rev. A* **53**, R19 (1996).
- [22] F. H. Mies, C. J. Williams, P. S. Julienne, and M. Krauss, *J. Res. Natl. Inst. Stand. Technol.* **101**, 521 (1996).
- [23] A. J. Moerdijk, H. Boesten, and B. J. Verhaar, *Phys. Rev. A* **53**, 916 (1996).
- [24] P. O. Fedichev, M. W. Reynolds, and G. V. Shlyapnikov, *Phys. Rev. Lett.* **77**, 2921 (1996).
- [25] E. A. Burt, R. W. Ghrist, C. J. Myatt, M. J. Holland, E. A. Cornell, and C. E. Wieman, *Phys. Rev. Lett.* **79**, 337 (1997).
- [26] E. Tiesinga, A. J. Moerdijk, B. J. Verhaar, and H. Stoof, *Phys. Rev. A* **46**, R1167 (1992).
- [27] D. Guéry-Odelin, J. Söding, P. Desbiolles, and J. Dalibard, *Optics Express* **2**, 323 (1998).
- [28] D. Guéry-Odelin, J. Söding, P. Desbiolles, and J. Dalibard, *Europhysics Lett.* **44**, 25 (1998).
- [29] J. Söding, D. Guéry-Odelin, P. Desbiolles, G. Ferrari, and J. Dalibard, *Phys. Rev. Lett.* **80**, 1869 (1998).
- [30] S. Kokkelmans, B. J. Verhaar, and K. Gibble, *Phys. Rev. Lett.* **81**, 951 (1998).
- [31] P. Leo, E. Tiesinga, P. Julienne, D.K. Walter, S. Kasecek, and T. Walker, *Phys. Rev. Lett.* **81**, 1389 (1998).
- [32] See however D. Boiron, A. Michaud, J.-M. Fournier, L. Simard, M. Sprenger, G. Grynberg, and C. Salomon, *Phys. Rev. A* **57**, R4106 (1998). In that experiment, cesium atoms have been confined in a laser trap at a peak density 10^{13} cm^{-3} , with a $1/e$ decay time $\sim 0.3 \text{ s}$. This puts the upper bound $1.5 \times 10^{-25} \text{ cm}^6 \text{ s}^{-1}$ on the 3-body rate coefficient.
- [33] M. H. Anderson, J. R. Ensher, M. R. Matthews, C. E. Wieman, and E. A. Cornell, *Science* **269**, 1989 (1995).
- [34] C. C. Bradley, C. A. Sackett, and R. G. Hulet, *Phys. Rev. Lett.* **78**, 985 (1997) ; see also C. C. Bradley, C. A. Sackett, J. J. Tollet, and R. G. Hulet, *Phys. Rev. Lett.* **75**, 1687 (1995).
- [35] K. B. Davis, M.-O. Mewes, M. R. Andrews, N. J. van Druten, D. S. Durfee, D. M. Kurn, and W. Ketterle, *Phys. Rev. Lett.* **75**, 3969 (1995).
- [36] A similar procedure, with slightly different fitting functions, is outlined in J. R. Ensher, D. S. Jin, M. R. Matthews, C. E. Wieman, and E. A. Cornell, *Phys. Rev. Lett.* **77**, 4984 (1996).
- [37] Y. Castin and R. Dum, *Phys. Rev. Lett.* **77**, 5315 (1996).
- [38] S. Giorgini, L. P. Pitaevskii, and S. Stringari, *Phys. Rev. A* **54**, R4633 (1996).